CO_2-SATURATED BRINE FLOODING: AN EFFECTIVE PROCESS FOR MOBILIZATION AND RECOVERY OF WATERFLOOD RESIDUAL OIL

A.H. Alizadeh[1], M.A. Ioannidis[2], M. Piri[1]
[1]Department of Chemical & Petroleum Engineering, University of Wyoming, Dept. 3295, 1000 E. University Ave., Laramie, WY 82071-2000, USA
[2]Department of Chemical Engineering, University of Waterloo, 200 University Ave. W., Waterloo, ON N2L 3G1, Canada

This paper was prepared for presentation at the International Symposium of the Society of Core Analysts held in Austin, Texas, USA 18-21 September, 2011

ABSTRACT

We present the results of an experimental study in which liberation of CO_2 gas from CO_2-saturated brine, as a result of pressure reduction, is employed to recover trapped oil left by waterflooding in a water-wet Berea core. It is shown that this novel process recovers more than 50% of the original trapped oil. A state-of-the-art core-flooding system is used to perform a two-stage flow experiment with a different level of CO_2 saturation in brine at each stage. The core, which was first saturated with fresh brine, was subjected to primary drainage by oil leading to 31.6% initial water saturation and then to a fully fresh-brine flood leading to 41% trapped residual oil saturation. Subsequently, brine saturated with CO_2 at 90.0 psig was introduced into the core at a constant inlet pressure. A sophisticated back pressure regulation system was utilized to tightly control and gradually reduce the outlet pressure of the core. The gradual increase in pressure drop across the system led to liberation of CO_2 from brine, three-phase flow and mobilization of oil ganglia. The process was continued until the outlet pressure reached 2 psig, at which oil saturation decreased down to 20%. The study was continued by repeating the above process at a higher level of CO_2 saturation in brine. To do so, the pressure in the sample was first increased to 180 psig to re-dissolve the CO_2 into the brine followed by injection of new brine, saturated with CO_2 at 180 psig, twice the level used in the first stage. The remaining oil saturation was further reduced to 17.3%, resulting in a cumulative recovery factor of 74.7%; 34.7% additional recovery of original oil in place (OOIP) compared to the initial waterflood. Parallel pore-scale visualization studies using transparent glass micromodels indicated that the effectiveness of the above approach is linked to the interaction between a flowing, disconnected gas phase and oil ganglia (three-phase ganglion dynamics).

INTRODUCTION

Waterflooding of oil reservoirs, first considered in 1880 [1], has been one of the most important oil recovery and pressure maintenance techniques [2]. Waterflood residual

(trapped) oil saturation, however, is high, typically 30-50% in water-wet systems. This has motivated significant amount of research on EOR techniques, aimed at recovery of the trapped oil. Pore-level displacement physics have been investigated using glass micromodels and microtomography techniques allowing design of effective enhanced recovery methods for reservoirs with various saturation histories and wettabilities. Micromodel experiments have been used to study mobilization of waterflood residual oil by gas injection under different wetting and spreading conditions [3,4] and displacement of residual oil by gravity-assisted gas injection [5,6]. Researchers have also used experiments in real porous systems to examine EOR effectiveness. Hustad and Holt [7] studied gravity stable displacement of oil by hydrocarbon gas after waterflooding, and Naylor *et al.* [8] investigated post-water flood depressurization for a field in North Sea. The effectiveness of the above-mentioned techniques was shown to depend on the formation of a "continuous" oil phase through, for instance, double displacement mechanisms and formation of spreading oil layers. In this manuscript, however, we investigate a novel EOR technique that relies on mobilization and recovery of waterflood residual oil as a *discontinuous* phase. The method is based on establishing conditions of *steady* exsolution and subsequent flow, as a *disconnected* phase, of CO_2 gas from injected carbonated brine [9-12]. Degassing is a non-equilibrium process driven by supersaturation of the aqueous phase in CO_2, namely by the condition $HC - Pw > 0$, where C and P_w are the *local* CO_2 concentration and pressure of the aqueous phase, respectively, and H is Henry's constant. In the application considered here, supersaturation results from viscous pressure drop associated with the flow of carbonated brine. We present here experimental evidence of very significant recovery of waterflood residual oil from a consolidated sandstone core and complement this finding with pore-scale visualizations revealing that the mechanism of recovery is the interaction of oil ganglia with a flowing, discontinuous gas phase (three-phase ganglion dynamics).

CORE SAMPLE AND FLUIDS

A core plug, 12" in length and 1.5" in diameter, was cut from a block of Berea sandstone using tap water as a coolant, and dried in an oven at 110 °C for 3 days and cooled in a desiccator for 2 days. The plug was then X-ray imaged using a medical CT scanner to investigate its homogeneity. The three-dimensional images of the sample showed that it was nearly homogeneous, save for a thin heterogeneous layer at one end. After trimming its end faces, the plug was divided into two pieces, a 10" core (sample A) used for the main experiment and a 1" piece (sample B) used for a reference scan. The 1" core was cut from the end that did not include the heterogeneous layer. Both samples A and B were then oven-dried and cooled as described above. The brine permeability of the core measured during the experiment was 89.08 mD and its average porosity determined using the CT scanner was 20.77%.

The aqueous phase was formulated using distilled water, 2 wt% of $CaCl_2$, 12 wt% of NaI, and 0.01 wt% of NaN_3 as a biocide. Brine density was 1.116 g/ml at atmospheric pressure and lab temperature (20°C). Mineral oil, Soltrol 170, was used as the oil phase. It was purified by passing it through dual-packed columns of silica gel and alumina to remove

polar contaminants, which might alter the water wetness of the rock. Iodooctane (5 vol%) was then dissolved in the purified Soltrol to obtain a working oil phase of density equal to 0.804 g/ml. All chemicals were reagent grade and used as received. CO_2 was used as the gas phase. It was withdrawn from a pressurized cylinder of 99% purity.

During the experiment, three-phase in-situ saturations were measured using the CT scanner. Sodium iodide and iodooctane were added as X-ray dopants to the aqueous and oil phases, respectively. The saturation measurements were carried out by scanning the sample at two energy levels, and hence concentration of the dopants were selected so that, in both energy levels, the contrast between CT numbers of each pair of fluids was large enough to allow the phases to be distinguished by the scanner. Further details regarding scanning parameters and procedures are provided later in this document.

The fluid system mentioned above was believed to be a spreading system even though the interfacial/surface tensions between the fluids were not measured. Nevertheless, when oil droplets were placed on brine in an open container in the presence of air (not CO_2), they immediately spread forming a thick layer sandwiched between air and brine.

EXPERIMENTAL APPARATUS

The experimental setup used in this study was a closed system composed of Hastelloy dual-cylinder Quizix pumps for injection and retraction of fluids at constant rate/pressure, differential pressure transducers, a 3500 ml three-phase separator, a Hassler-type core holder, and a medical CT scanner for in-situ saturation measurements. Figure 1 shows a detailed diagram of the flow system. The dual-cylinder pumps were used for injection of three fluids, i.e., brine, oil, and CO_2 (Pumps 1 to 3), back pressure regulation (Pump 4), overburden pressure maintenance (Pump 5), and separator pressure regulation (Pump 6). The fluids were injected into the core using Pumps 1 to 3 in Paired Constant Flow Rate (or Pressure) mode and received from the core by Pump 4 in Paired Constant Pressure Receive mode. The fluid injection pumps retracted fluids either from the separator or from open containers depending on the details of the experimental procedure. Also, Pump 4 discharged its fluids, received from the core, into either the separator or open containers. A separator pressure regulation system compensated for all the accumulations (positive or negative) using a large dual-cylinder pump (Pump 6) that allowed us to obtain very stable separator pressures leading to stable equilibrium between fluids. Rosemount differential pressure transducers were used to measure pressure drop across the core. A sophisticated control system was utilized to operate the pumps and log the data throughout the experiments. Finally, the medical CT scanner used could be rotated from horizontal to vertical orientation allowing flow tests through vertically- and horizontally-placed core samples. All the experiments presented in this paper were carried out with the core sample oriented vertically and at 20°C.

EXPERIMENTAL PROCEDURE

A key objective of the experiment was to assess the extent of recovery of waterflood residual oil by *in situ* gas exsolution from continuously injected carbonated brine during

pressure depletion. To do so, the established waterflood residual oil was surrounded by CO_2-saturated brine, and then pore-pressure was reduced using a highly controllable back-pressure regulation system allowing exsolution of the dissolved CO_2. One could consider doing this in both 'static' and 'dynamic' modes meaning with and without injection of additional CO_2-saturated brine. We have done the latter, seeking to achieve the maximum possible recovery of trapped oil. To this end, we used a long core sample of low permeability that could generate high pressure drop at relatively low brine flow rates leading to exsolution of maximum quantities of CO_2 from brine for a given back pressure. The core was placed in the core holder under overburden pressure and flooded with CO_2 gas to remove air. Then, the core was subjected to vacuum for a while followed by injection of fresh brine from the bottom of the core with a small flow rate to fully saturate the core with fresh brine. Fresh brine used in each step of the experiment was carefully deaerated. After obtaining brine reference scans (see below), the core was oil-flooded from the top to establish initial brine saturation and then waterflooded from bottom with fresh brine to establish residual oil saturation. Both of these steps were achieved at a highly stable back pressure of 90 psig. During primary oil drainage, oil flow rate was increased gradually to a maximum flow rate of 0.8 ml/min. This led to an average initial brine saturation of 31.6%. During subsequent waterflood, brine flow rate was increased very slowly to minimize undesirable dynamic effects on the maximum residual saturation that could be established. The maximum fresh brine flow rate used was 0.2 ml/min corresponding to capillary number of 1×10^{-6} and the average residual oil saturation obtained was 41%. The core was considered to be at the residual oil saturation when oil saturation did not change with increasing flow rate. In the oil flood, as in fresh brine flooding, the oil pump was retracting oil from a bucket because oil had not been added to the separator, as it did not need to be at equilibrium with CO_2 for the CO_2-saturated brine flooding (CSBF) step.

Prior to the experiment, relatively large volumes of the brine and CO_2 gas phases at equilibrium were prepared. The separator was first filled with fresh brine and CO_2 at 90 psig and both phases were recirculated through a bypass line in the system to reach equilibrium at 90 psig. The experimental setup was designed to release mixture of fluids, brought by Pump 4, at the bottom of the separator in both recirculation and main experiment, so the gas phase was bubbled through the liquid phase. To perform the CSBF process, it was decided to inject saturated brine from the bottom of the core while gradually decreasing the outlet pressure (initially at 90 psig). The back pressure was slowly and carefully decreased to allow the saturated brine to release its CO_2 according to the local pressure across the core. The exsolution of CO_2 led to a gradual increase in pressure drop across the core and hence a chance to reduce the inlet flow rate, which had to be increased little in order to compensate temporary pressure drops in the core inlet resulted from the back pressure reduction.

The CSBF process was performed using constant rate mode. Saturated brine was injected from the bottom of the core for one pore volume at 0.05 ml/min flow rate. This low flow rate ensured no oil mobilization prior to pressure depletion. Subsequently, the back

pressure, initially set at 90 psig, was reduced in small increments. The slow reduction in back pressure was continued until the inlet pressure reached close to 90 psig, when gas was allowed to completely come out. Since liberation of gas enhanced the differential pressure and caused the inlet pressure to increase for a given flow rate, it gave us the opportunity to decrease the back pressure further to bring the inlet pressure down again to 90 psig. This approach was continued and the fluid saturations were measured regularly to follow possible variations in oil saturation. One difficulty encountered in the saturation measurement was that although the measurements confirmed a gradually descending trend in oil saturation during saturated brine flooding, oil saturation slightly oscillated if measurements were made in short time intervals. This difficulty was due to the fact that, since the core had to be scanned at two different energy levels, the distribution of each fluid between two successive scans was not stationary due to the inherently dynamic nature of the experiment. In this experiment, steady-state for a given brine flow rate and pressure drop was achieved after a relatively long time. The experiment was continued by decreasing back pressure and adjusting the flow rate (to increase or decrease the inlet pressure) until the back pressure reached about 2 psig, i.e., a pressure drop of 88 psig. It should be noted that during this process, the injection flow rate was never allowed to increase above values corresponding to capillary numbers greater than 1×10^{-6}. At the end of this process, to determine the true oil saturation distribution in the core and resolve the difficulty described earlier, the outlet pressure was gradually increased, while injecting brine, to dissolve the "free" CO_2 back into the brine. When back pressure reached 90 psig, the pressure of the entire system was, in one increment, increased to 180 psig accelerating CO_2 dissolution. During this step, a large number of pore volumes of brine were injected at a low flow rate (< 0.2 ml/min). The sample was scanned several times to make sure that there was no gas present before reporting oil saturation. The values were nearly consistent with the oil saturations measured during three-phase flow. Dissolving CO_2 back into brine also eliminated possible effects of pressure variation on gas CT numbers.

In order to investigate if the injection of brine saturated with CO_2 at higher pressure could further decrease the new oil saturation (20%), the experiment was continued with new brine, saturated with CO_2 at 180 psig. This meant that we had to inject brine at 180 psig and establish higher pressure drops (higher differential pressures) in the same core to increase CO_2 exsolution. As in the previous step, brine and CO_2 were re-circulated and after achieving equilibrium at 180 psig, the experiment was resumed with the same procedure as before. The only difference with the previous step was that the constant pressure mode was selected to operate the brine pump, as more insight into possible variations of the injection flow rate had been developed. The back pressure was decreased gradually from 180 psig to 17 psig. At the end of this step, the pressure of the system was increased to 360 psig to dissolve the free CO_2 and determine the oil distribution along the core.

POROSITY AND IN-SITU SATURATION MEASUREMENTS

The scanner provided 250 μm resolution per slice and a minimum slice thickness of 1 mm. Porosity was calculated from:

$$\varphi = \frac{CT_{wc} - CT_{gc}}{CT_w - CT_g} \quad (1)$$

where CT_{wc} and CT_{gc} are CT numbers of the core fully saturated with brine and gas, respectively. CT_w and CT_g were obtained by scanning the core holder filled with only brine or gas, respectively. Figure 2a shows the slice-averaged porosity distribution along sample A determined using the above-mentioned technique. The figure presents values for 22 slices equidistant along the length of core. Each value represents porosity of one slice perpendicular to the core axis with 2 mm thickness. The distribution confirms homogeneity of the sample observed already from the dry scan. As it is seen in this figure, porosity slightly increases at the bottom of the core where higher attenuations were observed. Overall, the variation in porosity is insignificant. The mean porosity, which is the average of all the slices, is 20.77%. This value is consistent with an independent measurement of porosity on another core sample cut from the same block of Berea sandstone. To calculate three phase saturations, the core was scanned at two different energy levels during the experiment and also when it was fully saturated with each of the fluids (to obtain reference scans). Saturations were then determined by obtaining a simultaneous solution for the following system of equations:

$$S_w = \frac{(CT_{c2} - CT_{gc2})(CT_{oc1} - CT_{gc1}) - (CT_{c1} - CT_{gc1})(CT_{oc2} - CT_{gc2})}{(CT_{oc1} - CT_{gc1})(CT_{wc2} - CT_{gc2}) - (CT_{oc2} - CT_{gc2})(CT_{wc1} - CT_{gc1})} \quad (2)$$

$$S_o = \frac{(CT_{c1} - CT_{gc1})(CT_{wc2} - CT_{gc2}) - (CT_{c2} - CT_{gc2})(CT_{wc1} - CT_{gc1})}{(CT_{oc1} - CT_{gc1})(CT_{wc2} - CT_{gc2}) - (CT_{oc2} - CT_{gc2})(CT_{wc1} - CT_{gc1})} \quad (3)$$

$$S_g = 1 - S_w - S_o \quad (4)$$

where CT_{c1} and CT_{c2} are the CT numbers of the core containing all phases at energy levels 1 and 2, respectively. In order to calculate saturations in a three-phase system, the core must be scanned at two energy levels when fully saturated with each of the fluids, in order to obtain the reference scans. For the gas reference scan, the core was mounted in the core holder under overburden pressure and then vacuumed. The overburden pressure in all steps of the experiment was 250 psi higher than the inlet pore pressure. After vacuuming the core for a while to remove bulk air, CO_2 was introduced into the core and the fully CO_2-saturated core was scanned at two energy levels (130 keV with 100 mA and 80 keV with 125 mA) and at two different pore pressures, 0 and 90 psig. All the scans were obtained with 2 mm slice thickness and 11 mm index. The two sets of CT numbers obtained were very similar. Then, the core was fully saturated with fresh brine, as pointed out in the previous section, and scanned at 0 and 90 psig pressures at both energy levels. We did not observe any differences between the CT numbers of the scans at two pressures, which was expected for an incompressible liquid phase.

Since the density of brine slightly increases by dissolution of CO_2, it was decided to scan the core with CO_2-saturated brine as well. Therefore, fresh brine in the core was replaced by CO_2-saturated brine through miscible displacement. The back pressure during this process was maintained at 90 psig to avoid exsolution of CO_2 from brine in the core. After injecting a large number of pore volumes of saturated brine, the core was scanned. Interestingly, the CT numbers of the core in both fresh brine and saturated brine cases were nearly identical. The core was then flooded with copious amounts of deaerated fresh brine at high flow rates and at 90 psig as back pressure to flush out CO_2-saturated brine from the core. However, after re-saturating the core with fresh brine, the outlet pressure of the core at other subsequent steps, including primary oil drainage and fresh brine imbibition, was maintained at 90 psig to insure that no possible remaining CO_2 could exsolve into the pore space in the core before initiating the CSBF process.

The only reference scan left at this stage was the one with fully oil-saturated core. To saturate the core with oil, brine must be flushed out by a solvent such as isopropyl alcohol. However, because of high concentration of salts, the direct displacement of brine with isopropyl alcohol could cause salt precipitation. As a result, the high-salinity brine must be first flushed out by low-salinity brine and then the diluted brine must be displaced by the solvent. Since this process is time consuming, it was decided to use a smaller core to obtain the oil reference scan. Accordingly, as mentioned earlier, a small piece (sample B) of the original core plug was used to make sure that the oil reference scan was representative of the 10" core (sample A). Sample B was saturated with oil using the above-mentioned procedure and then scanned at different locations along its length. The CT numbers were then averaged and used in three-phase saturation calculations presented here.

RESULTS AND DISCUSSION

Figure 2b shows the distribution of initial brine and waterflood residual oil saturations along the core. As expected, brine saturation was higher at the outlet during primary oil drainage due to capillary end effects. At the end of primary oil drainage the average brine saturation was about 31.6%. This is mainly the brine left in the crevices and small pores, as the sample is believed to be strongly water wet. Subsequent water imbibition was carried out with 0.2 ml/min flow rate and a capillary number of 1×10^{-6} leading to an average residual oil saturation of 41%. To insure that oil was completely trapped, the flow rate was doubled, but no appreciable change was observed in the oil saturation distribution. The trapped oil resides in large pores, as it is the non-wetting phase, and is surrounded by fresh brine. Figure 3 presents selected CT slices along the length of the core and their respective average saturations for both drainage and imbibition processes. The images exhibit a fairly uniform distribution of fluids that is an indication of both homogeneity of the core and also capillary dominated displacements.

Initial injection of CO_2-saturated brine, i.e., without CO_2 exsolution, leads to miscible displacement of fresh brine. The CO_2-saturated brine comes in contact with all clusters of trapped oil in the core. Subsequent exsolution of CO_2 leads to contact of CO_2 gas with the

majority of trapped oil – a key advantage of this EOR method relative to gas injection processes during which gas has to first displace brine before gaining access to the trapped oil. Figure 4 compares CT slices of the core and their respective oil saturation at the end of fresh brine imbibition to those at the end of the first and second CSBF processes, after CO_2 was dissolved back into brine. It is shown that the first CSBF was able to recover about 51% of the original waterflood trapped oil reducing the oil saturation to about 20%. This is a remarkable reduction in trapped oil saturation. Figure 4 also shows the oil saturation at the end of second CSBF process (third row). This step does not lead to significant reduction in oil saturation. The average residual oil saturation was about 17.3% leading to an additional recovery of about 4% OOIP compared to the first stage. In other words, higher differential pressure drop was not able to further reduce oil saturation. This point may be important from economic and operational points of view. Namely, the majority of incremental oil recovery takes place at a lower level of CO2 saturation in brine. The slice-averaged oil saturation along the length of the core at the end of fresh brine imbibition, and CO2-saturated brine flooding at 90 and 180 psig inlet pressures are exhibited in Figure 5. The difference between the two top distributions again highlights the success of the first CSBF process in recovering the waterflood residual oil.

Figures 6a and 6b depict variations of pressure drop across the core with time and also with oil saturation for the first CO_2-saturated brine flooding. Pressure drop increases significantly as oil is recovered and as back pressure is reduced. Even though recovery of oil acts to reduce the pressure drop, exsolution of CO_2 significantly increases it. This is mainly due to the fact that CO_2 occupies the largest pores and throats as the most non-wetting phase causing major blockage for the flow. This completely dominates the trend observed in the pressure drop. It is also shown that about 25% of the original waterflood residual oil was recovered with approximately 60 psi pressure drop, 68% of the maximum pressure drop achieved, while the next 25% was recovered by only 28 psi more pressure drop, totaling 88 psi. In other words, recovery of oil did not follow a linear relationship with pressure drop across the core in CSBF process and was more efficient at the late stages of the process.

MICROMODEL EXPERIMENTS

Exsolution of CO_2 from a locally supersaturated aqueous phase in porous media begins with heterogeneous gas bubble nucleation and leads to *steady-state gas cluster dynamics* (growth, mobilization, fragmentation, collision and coalescence) [9,10]. When oil ganglia are also present, the flowing, albeit disconnected, gas phase sets up a cascade of double drainage and double imbibition displacements during which parts of large oil clusters or small oil ganglia are gradually mobilized with the gas phase (Figure 7). Steady-state gas cluster dynamics means each pore is visited by gas a great number of times. The efficiency of oil recovery at the pore scale is related to the local intensity of gas phase dynamics. Additional pore scale visualizations with non-spreading oils (data not shown) reveal that the effectiveness of the process is insensitive to the ability of oil to spread in

the presence of gas. In all visualization studies, however, oil is the intermediate wetting phase and this appears to be important to the success of the process.

CONCLUSIONS

Significant reduction (>50%) in waterflood residual oil, yielding more than 30% OOIP additional recovery, was obtained in a low-permeability water-wet Berea sandstone core using a novel EOR process based on injection of CO_2-saturated brine. Steady-state gas cluster dynamics, a consequence of continuous in-situ degassing, was visually observed to be responsible for the recovery of trapped oil, at brine injection flow rates corresponding to capillary-dominated displacement. Notably, this process may offer the possibility for EOR with simultaneous CO_2 sequestration.

ACKNOWLEGMENT

We gratefully acknowledge financial support of EnCana, Saudi Aramco, the School of Energy Resources and the Enhanced Oil Recovery Institute at the University of Wyoming.

REFERENCES

1. Carll, J.F., "The Geology of the Oil Regions of Warren, Venango, Clarion and Butler Counties," Pennsylvania Second Geological Survey, Report III, (1880), 263.
2. Willhite, G.P., *Waterflooding*, Society of Petroleum Engineers, Richardson, Texas, (1986), 550.
3. Oren, P.E., J. Billiotte, and W.V. Pinczewski, "Mobilization of Waterflood Residual Oil by Gas Injection for Water-Wet Conditions," *SPE Formation Evaluation*, (1992) **7**, 1, 70-78.
4. Oren, P.E. and W.V. Pinczewski, "The Effect of Wettability and Spreading Coefficients on the Recovery of Waterflood Residual Oil by Miscible Gasflooding," *SPE Formation Evaluation*, (1994) **9**, 2, 149-156.
5. Kantzas, A., I. Chatzis and F.A.L. Dullien, "Mechanisms of Capillary Displacement of Residual Oil by Gravity-Assisted Inert Gas Injection," Paper SPE 17506 presented at the SPE Rocky Mountain Regional Meeting, Casper, WY, May 11-13, 1988.
6. Chatzis, I., A. Kantzas, A. and F.A.L. Dullien, "On the Investigation of Gravity-Assisted Inert Gas Injection Using Micromodels, Long Berea Sandstone Cores, and Computer-Assisted Tomography," Paper SPE 18284 presented at the 63rd Annual Technical Conference and Exhibition, Houston, TX, October 2-5, 1988.
7. Hustad, O.S. and T. Holt, "Gravity Stable Displacement of Oil by Hydrocarbon Gas After Waterflooding," Paper SPE 24116 presented at the SPE/DOE 8th Symposium on Enhanced Oil Recovery, Tulsa, OK, April 22-24, 1992.
8. Naylor, P., T. Fishlock, D. Mogford and R. Smith, "Relative Permeability Measurements for Post-Waterflood Depressurization of the Miller Field, North Sea," *SPE Reservoir Evaluation and Engineering*, (2001) **4**, 4, 276-280.

9. Zhao, W. and M.A. Ioannidis, "Gas exsolution and flow during supersaturated water injection in porous media: I. Pore network modeling," *Advance in Water Resources*, (2011) **34**, 1, 2-14.
10. Enouy, R., M. Li, M.A. Ioannidis and A.J.A. Unger, "Gas exsolution and flow during supersaturated water injection in porous media: II. Column experiments and continuum modeling," Advance in Water Resources, (2011) **34**, 1, 15-25.
11. Nelson, L., J. Barker, T. Li, N. Thomson, M.A. Ioannidis and I. Chatzis, "A field trial to assess the performance of CO2-supersaturated water injection for residual volatile LNAPL recovery," *Journal of Contaminant Hydrology*, (2009) **109**, 1-4, 82-90.
12. Li, T.M.W., M.A. Ioannidis and I. Chatzis, "Recovery of non-aqueous phase liquids from ground sources," United States patent #7300227, (2007).

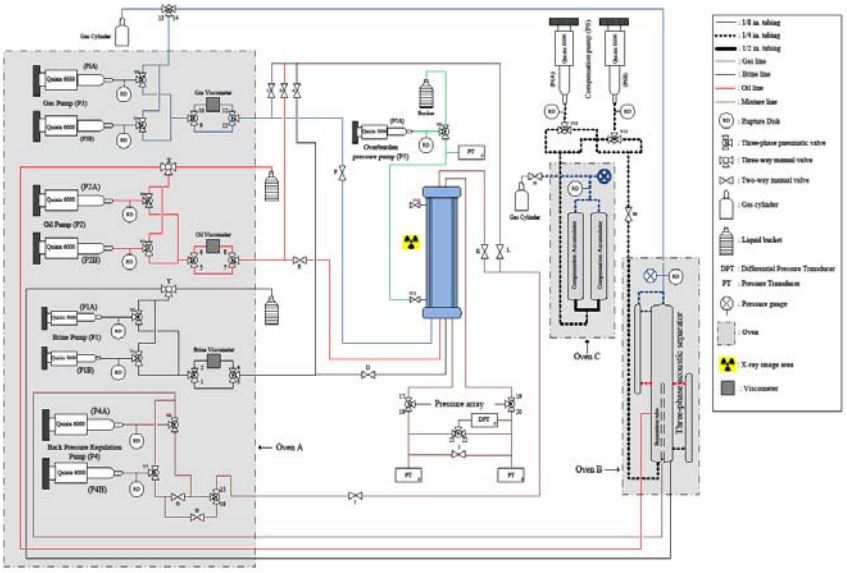

Figure 1. Experimental apparatus used in this study.

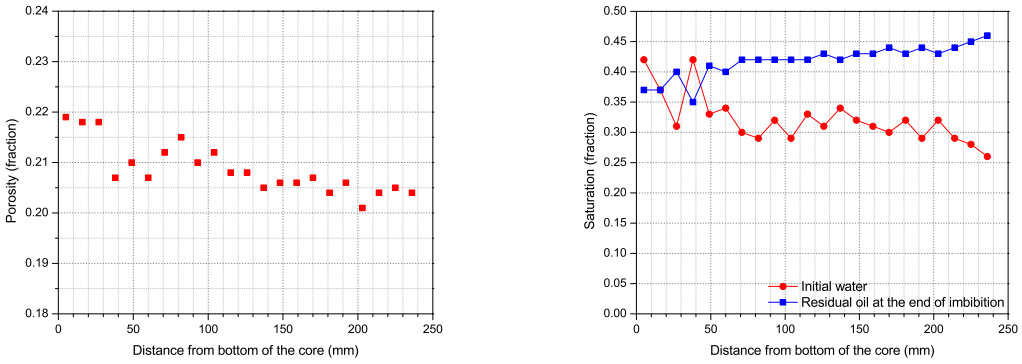

(a) (b)

Figure 2. (a) Slice-averaged porosity distribution along the length of the core measured using x-ray imaging. (b) Slice-averaged saturations along the length of the core at the end of primary oil drainage and water imbibition.

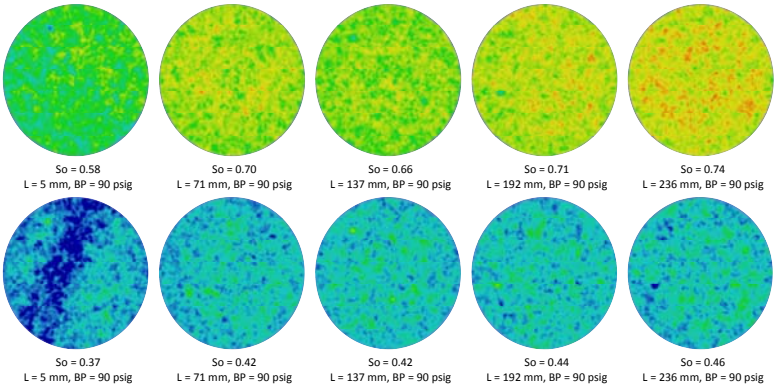

Figure 3. CT images showing oil saturation distribution at the end of primary drainage (first row) and at the end of imbibition (second row). L represents the distance of the slice center from bottom of the core. (S_o = 0  S_o = 1).

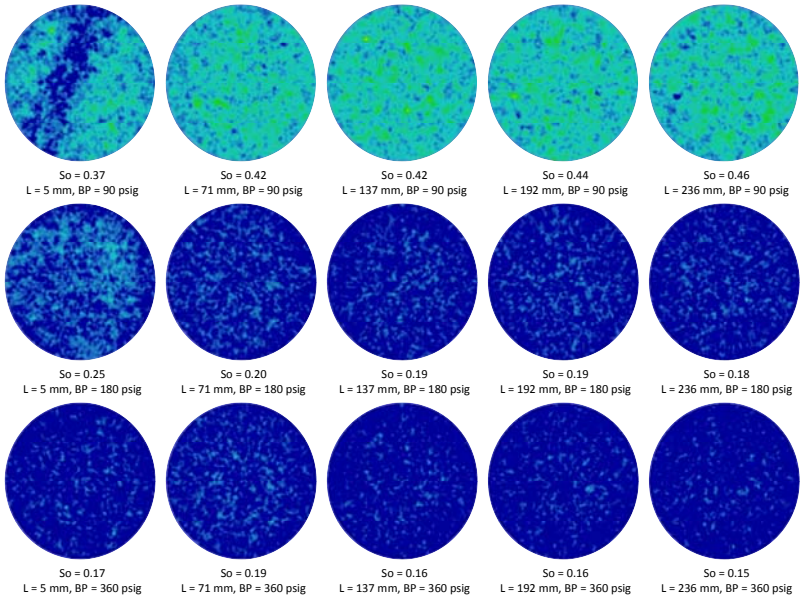

Figure 4. CT images showing oil saturation distribution at the end of imbibition (first row), first saturated-brine flooding (second row) and second saturated-brine flooding (third row). L represents the distance of the slice center from bottom of the core. (S_o = 0  S_o = 1).

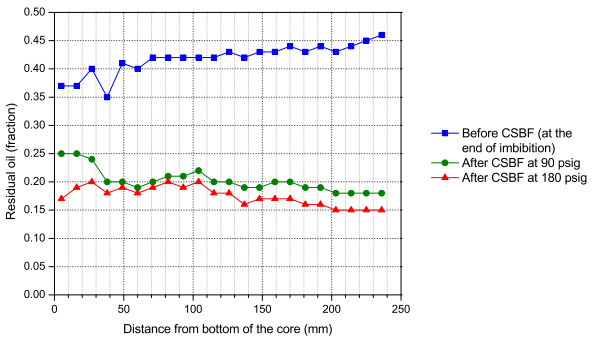

Figure 5. Slice-averaged residual oil saturation along the length of the core at the end of fresh brine imbibition, and CO_2-saturated brine flooding at 90 and 180 psig inlet pressures.

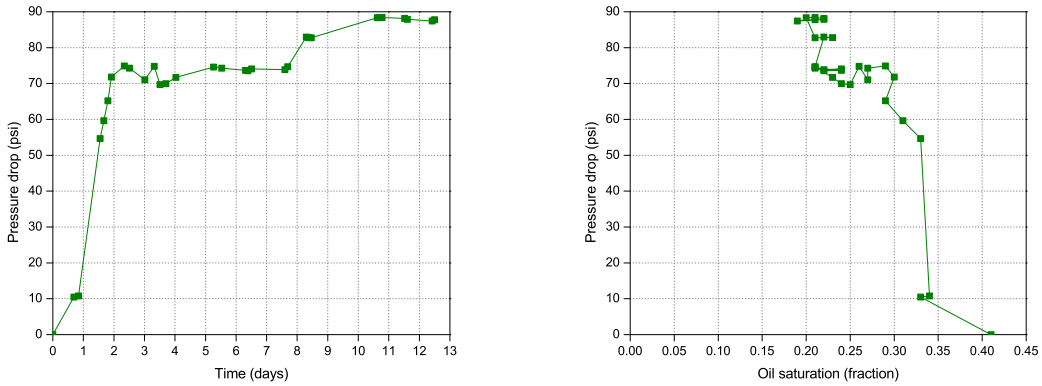

(a) (b)

Figure 6. (a) Variation of pressure drop across the core with time for the first CSBF. (b) Variation of pressure drop across the core with residual oil saturation for the first CSBF.

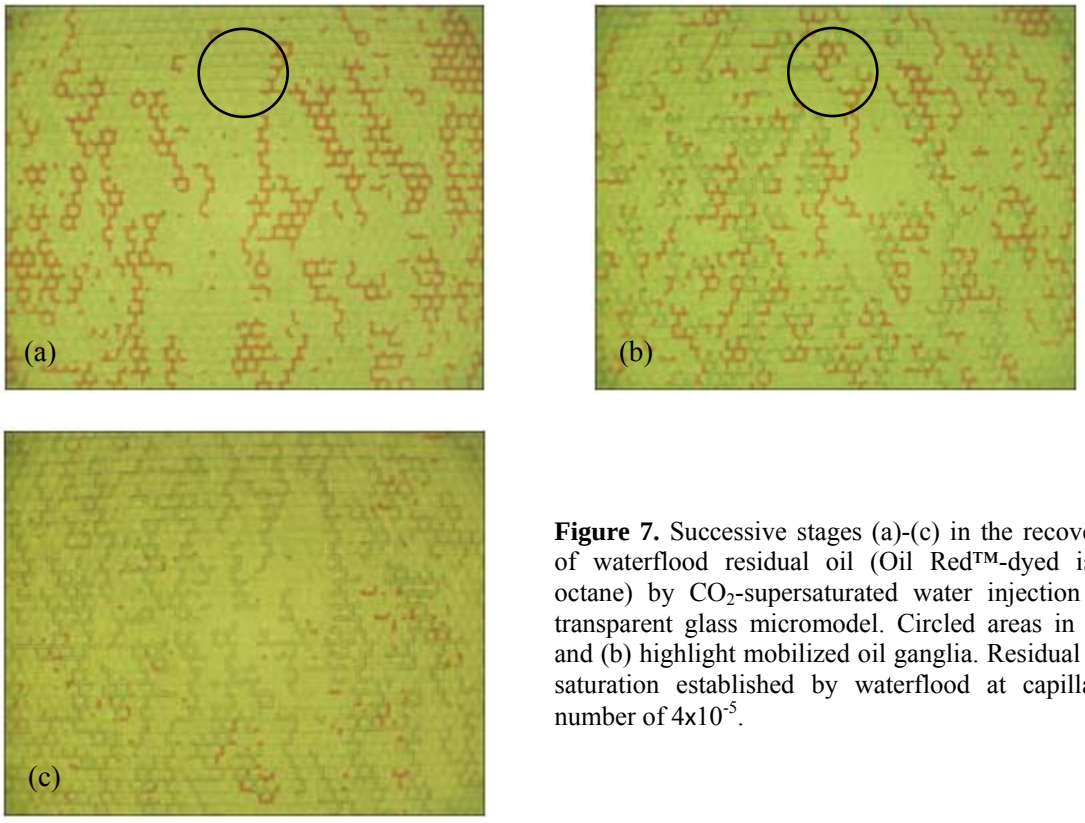

Figure 7. Successive stages (a)-(c) in the recovery of waterflood residual oil (Oil Red™-dyed iso-octane) by CO_2-supersaturated water injection in transparent glass micromodel. Circled areas in (a) and (b) highlight mobilized oil ganglia. Residual oil saturation established by waterflood at capillary number of $4x10^{-5}$.